

## Research Article

## Open Access

Anil Kumar and Sevi Murugavel\*

# Influence of textural properties on biomineralization behavior of mesoporous bioactive glasses

DOI 10.1515/bglass-2015-0002

Received 8.01.2015; accepted 12.04.2015

**Abstract:** A new method of calcination for the sol-gel derived bioactive glass sample has been developed to produce superior textural and bioactive properties. Based on this method, mesoporous 67.4 SiO<sub>2</sub>-25 Na<sub>2</sub>O-5 CaO-2.6 P<sub>2</sub>O<sub>5</sub> (mol.%) bioactive glasses (MBGs) have been synthesized through acid assisted sol-gel technique followed by evaporation induced self-assembly (EISA) process, commonly used for obtaining bioactive glasses. Moreover, the use of microwave irradiation has been compared with that of conventional heat treatment for a particular quaternary composition, which has allowed the homogeneous spatial distribution of heat and to obtain smaller, uniform pore sizes with high surface area. The distinctions between the two methods of calcination have been observed in the structural, morphology and textural characteristics. The superior textural characteristics have allowed the rapid dissolution of MBGs followed by development of nanocrystalline hydroxycarbonate apatite (HCA) layer. *In vitro* bioactive analyses on both MBGs have revealed a rapid formation HCA layer with distinct behavior on the biomineralization process. The difference in the behavior of biomineralization process is attributed to the kinetics of supersaturation of the biological medium.

**Keywords:** Bioactive glass, Microwave irradiation, Bioactivity, EISA, SBF

## 1 Introduction

Bioactive glasses (BGs) in biomedical applications are becoming increasingly important, which shows adequate

response with the bone healing process, cell tissue (tissue engineering), and material cell interaction. This is the juncture where invention of a new kind of material is highly desired which demonstrates proper regenerative capacity by stimulating genes and initiating bone healing and other bio-functionalities. The most interesting behavior of BGs as bioactive systems is that it bonds with bone rapidly and also stimulates bone growth away from the bone-implant interface [1]. In recent years, different studies have shown that the BGs exhibit unique properties such as osteoconduction and osteostimulation behavior in comparison with other classes of biomaterials [2]. There is a formation of thin carbonated hydroxyapatite (HCA) layer when they are exposed to biological fluid. The HCA layer formation is caused by the exposure of BG into biological fluid leading to dissolution of glass surface followed by sequential rapid chemical reactions. In general, the HCA layer have the same chemical composition as that of mineral component of human bone and it has strong tendency to bond with human organism and stimulate the bone healing mechanism. Among the various glass compositions investigated in the literature over last four decades, one of the most widely studied BG is the bioactive silicate “45S5 Bioglass” and found to show the excellent bone bonding ability [3–5].

Over the decades, several attempts have been made to design new BGs with an aim towards equal or better bioactivity than 45S5 glass. In particularly, the synthesis of porous BGs with tailored porosity and suitable mechanical properties by various routes such as sol-gel foaming, foam replication, electro-spinning, ice-templating and 3-D scaffold structures [6–9]. Among the various methods of preparation, the sol-gel glasses are found to possess sufficient pores in the network structure and it shows the excellent dissolution rate and rapid formation of HCA layer than the corresponding melt derived glass [10]. In addition to its exceptional bioactive characteristics, the BGs could also be used as matrices for the local drug delivery system [11]. Therefore, it is important to optimize both pore architecture and morphology of BGs, which brings various

\*Corresponding Author: Sevi Murugavel: Department of Physics and Astrophysics, University of Delhi, Delhi-110007, India, E-mail: murug@physics.du.ac.in

Anil Kumar: Department of Physics and Astrophysics, University of Delhi, Delhi-110007, India

functionalities for their use as biomaterials in advanced tissue engineering applications. The synthetic methodology for fabrication of hierarchically porous BGs for the bone tissue regeneration has been developed by various research groups over the years [12–15]. Porous bioactive glasses have a well interconnected pore structure in the size ranging between few nano meters and micron meters depending on the chemical constituents and synthesis conditions. In this direction, new developments have been made for synthesizing mesoporous bioactive glasses by adopting various routes, which lead us to control the textural properties. The newest approach is the evaporation induced self-assembly (EISA) process, which involves the use of surfactant as structure directing agent (SDA) [16, 17]. Within this process, non-ionic block copolymers are used as SDA whose unique self-assembling properties allow us to obtain ordered mesoporous structures. The ordering properties of copolymers can be altered by changing solvent composition, molecular weight, temperature, medium of reaction and copolymer architecture. Based on the EISA process, different BG compositions containing alkali-alkaline earth oxide have been synthesized and characterized by various techniques including *in vitro* behavior [18–21].

The glasses prepared by the EISA process undergoes the different stages before it reaches the final product such as formation of sol- followed by gel, aging of the gel subsequent drying process. After the drying event, the obtained reactant powders are calcinated to remove the unwanted precursor materials, which are taken in the precursor material and hence the calcined temperature decides particularly the textural properties and uniquely the glassy nature. Therefore, it is important to optimize the calcination temperature which would provide suitable pore architectures followed by favorable biological response when it is exposed into biological medium. The enhanced bioactivity of porous BGs strongly depends on their high ion dissolution kinetics followed by enhanced biomineralization process [22]. More commonly, the calcination of reactant has been carried out by using conventional heating or electric furnace heating method above 500°C. During this process, the heat is transmitted into the medium from external source which leads to the occurrence of thermal gradient in the reactant. Additionally, the inhomogeneous temperature distribution can also lead to destruction of pore structure as well as loss of glassy nature.

The microwave heating method provides an alternative route to carry the calcination process and to obtain the reactant product without the destruction of pore architecture. Traditionally, the microwave process technique has been successfully applied to fabricate conventional

ceramics, in particularly nano sized ceramics in the past decades. This technique has several advantages over the conventional sintering and/or calcination process, such as low sintering temperature, homogenous temperature distribution and shorter processing time. Therefore, we extended the microwave heating technique, for the first time; to calcinate the sol-gel prepared bioactive silicate glass to enhance textural characteristics. In this work, we report the synthesis, characterization and to study the *in vitro* behavior of quaternary silicate glass composition by conventional method of calcination and microwave-mediated metathesis process. As prepared glasses were characterized by various analytical techniques and its morphology has been analyzed by scanning electron microscopy. The microwave calcined sol-gel glass sample shows the superior textural characteristics and distinct biomineralization behavior than the conventional calcined glass sample.

## 2 Experimental Methods

### 2.1 Materials and sample preparation

Glass composition containing 67.4 SiO<sub>2</sub>-25 Na<sub>2</sub>O-5 CaO-2.6 P<sub>2</sub>O<sub>5</sub> (mol.%) has been derived through acid assisted sol-gel technique [23]. The precursors used for processing the bioglass as follows: Tetraethyl Orthosilicate (TEOS), Si(OC<sub>2</sub>H<sub>5</sub>)<sub>4</sub>, reagent grade, 98%; Triethyl Phosphate (TEP), (C<sub>2</sub>H<sub>5</sub>)<sub>3</sub>PO<sub>4</sub>, ≥99.8%; Sodium Acetate (NaAc), CH<sub>3</sub>COONa, ≥99.0%; Calcium Acetate hydrate (CaAc), (CH<sub>3</sub>COO)<sub>2</sub> Ca·xH<sub>2</sub>O, reagent grade, ≥99% were used from Sigma Aldrich. Non-ionic amphiphilic triblock copolymer EO<sub>20</sub>PO<sub>70</sub>EO<sub>20</sub> (Pluronic® P123) used as template or structure directing agent (SDA); Reagent grade triple deionized water (Avarice). Both TEOS and TEP generally involves in hydrolysis under acidic condition, polymer condensation in forming inorganic silica network respectively. The synthesis part includes immersion of TEOS, TEP, NaAc, and CaAc in some specific molar ratio in accordance with SiO<sub>2</sub>, P<sub>2</sub>O<sub>5</sub>, Na<sub>2</sub>O and CaO respectively in ethanol as a solvent at every one hour interval. The mixture was stirred at room temperature for 24 hours to undergo the homogenization for the gelation process. In addition, the 4 g of P123 polymer were dissolved in 60 g of ethanol before mixing the inorganic precursors keeping the constant ratio of (TEOS/TEP):Ethanol::1:4, (TEOS/TEP):Water::1:4 (Molar ratio); Water:Acid::1:6 (Weight ratio) [20, 21]. As prepared sol was then introduced into Borosil petridish for evaporation induced self-assembly (EISA) process followed by

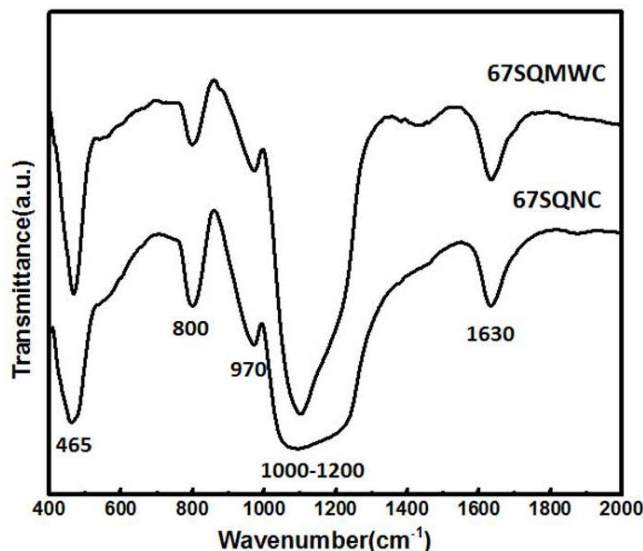


**Figure 1:** FTIR spectra of 67SQNC and 67SQMWC glass sample after the calcination process.

aging for 3 days at 80°C and then drying for 48 hours at 100°C.

Furthermore, during the acid treatment process, 1 g of resultant sample is mixed with 100 ml of sulphuric acid (48 wt.%) for 24 hours at 95°C following the procedure described elsewhere [24]. In addition, the resulting admixture was washed with distilled water and then with acetone until sample gets isolated from other residues and impurity. The final product was then calcined at 370°C by using both Micro Heat-High Performance Microwave Furnace (Enerzi Microwave System) and conventional heating method. Therefore, the nomenclature used for the glass sample calcined by conventional heating and microwave heating methods 67SQNC and 67SQMWC respectively. An obtained powdered glass sample was then analyzed by using X-ray diffraction (XRD) technique with MiniFlex2 (Rigaku 600) equipped with CuK $\alpha$  radiation for  $2\theta$  range of 10° to 60° having step size of 0.02 and scan speed of 2 °/min. FTIR spectroscopy (NICOLET 380) has been used to record the vibrational modes present in the as prepared glass and SBF soaked samples (NICOLET 380 FTIR spectroscopy). The FTIR spectra were run on the KBr pellets with weight ratio of sample to KBr of 1:100 with the spectral resolution of 4 cm<sup>-1</sup>. The morphology of the as prepared porous glass and SBF soaked glass sample was then analyzed by FESEM (MIRA3 TESCAN) machine having accelerating voltage of 30.0 kV and the resolution of 6 nm. Furthermore, the pristine glass morphology was characterized by the FEI Tecnai<sup>TM</sup> Transmission Electron Microscope (TEM) (TECNAI G<sup>2</sup> T30 U-TWIN) and had been attached with a double-tilt holder ( $\pm 70^\circ$ )

along with an EDX analyzer under an accelerating voltage of 300 kV (with the resolution of 0.19 nm). The images were recorded using a CCD camera (Gatan) and Fourier transform (FT) patterns have been conducted using a digital micrograph (Gatan). The textural property of the glass sample was characterized by nitrogen adsorption/desorption technique with Quantachrome, Autosorb-1C TCD analyzer (Model: ASIC-X-TCD6) and with the adsorptive gas of nitrogen, N<sub>2</sub> (cross sectional area of 0.162 nm<sup>2</sup>). Before the analysis, the porous glass sample was degassed under the vacuum for 6 h at 200 °C. The surface area and pore-size distribution has been determined by Brunauer-Emmett-Teller (BET) followed by Barret-Joyner-Halenda (BJH) method.

## 2.2 Assessment of the *in vitro* bioactivity

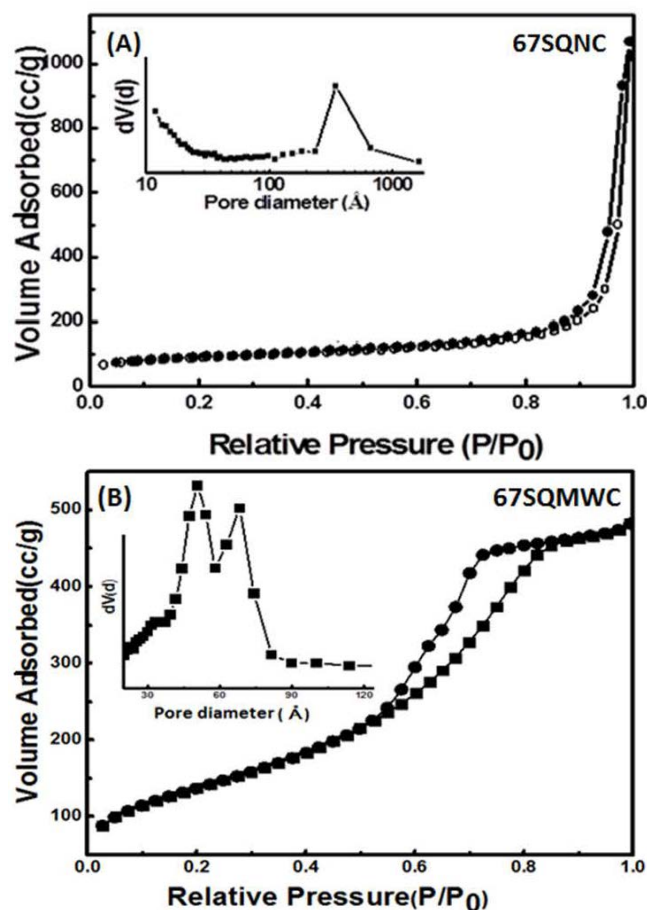
The *in vitro* bioactivity of as synthesized glass sample was carried out by immersing in SBF solution following the procedure proposed by Kokubo [25]. We have prepared SBF solution that has a similar composition and concentration to those of the inorganic part of the human plasma. For this purpose, we used Hanks' Balanced salt solution, HBSS (Sigma); TRIS (Hydroxymethyl) Aminomethane (SISCO research laboratory Pvt. Ltd, SRL) under desired proportion or by adjusting the pH to 7.75 to 7.85 at 22°C. The weighed amount (1 mg) of glass sample was immersed in 1mL of SBF solution [23] and stored in polyethylene bottle enclosed with air tight lid. The bottles were placed in an ORBITEK shaker (Scigenics Bio-tech) at a constant speed of 160 rpm at 37°C for the period of 1, 2, and 3 days. After soaking the glass samples in the SBF, the powders were collected by filtration subsequently air dried at room temperature.

## 3 Results

As synthesized glasses are characterized by powder XRD method and confirmed to be amorphous by observing a broad hump. Furthermore, we have carried out FTIR investigations on both the glass samples to understand the local structure by correlating the intrinsic vibrational modes. In Figure 1, we compare the FTIR spectra of both glass samples, which show the distinct behavior in the vibrational frequency and their intensity level, *i.e.* the characteristic bands are sharper in the case of microwave treated sample than the normal heat treated. In addition, there are few vibrational modes which become more visible in the case of microwave treated glass sample than the normal calcined sample. The FTIR spectra of as prepared glass

**Table 1:** Textural parameters of 67.4 SiO<sub>2</sub>-25 Na<sub>2</sub>O-5 CaO-2.6 P<sub>2</sub>O<sub>5</sub> (mol.%) glass

Sample	Surface area (m <sup>2</sup> /g)	Pore volume (cm <sup>3</sup> /g)	Pore diameter (nm)
67SQNC	308.6	1.46	34.9
67SQMWC	497.1	0.7484	5.07, 6.819

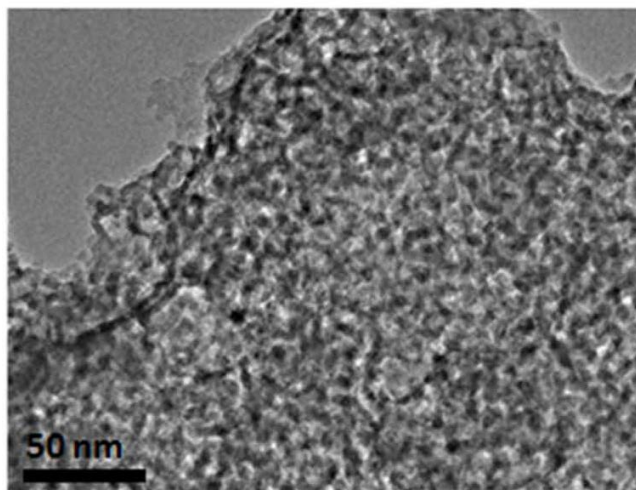
**Figure 2:** Nitrogen adsorption–desorption isotherm and pore size distribution (inset) of (A) 67SQNC (B) 67SQMWC glass samples in their pristine form

samples indicate that it exhibits the characteristic bands due to the Si-O vibrational modes: Si-O-Si stretch, Si-O bending, Si-O rocking and Si-O alkali stretching. The absorption band close to 1630 cm<sup>-1</sup> is attributed to the hydroxyl group, *i.e.*, surface silanols formed due to the adsorption of water molecules owing to the large porosity and high surface area. Furthermore, this band consists of the superposition of stretching modes of non-hydrogen-bonded silanols (isolated silanol groups) and hydrogen-bonded silanol (vicinal or germinal silanol groups) [26]. The broad bands in the region 1000 – 1200 cm<sup>-1</sup> cor-

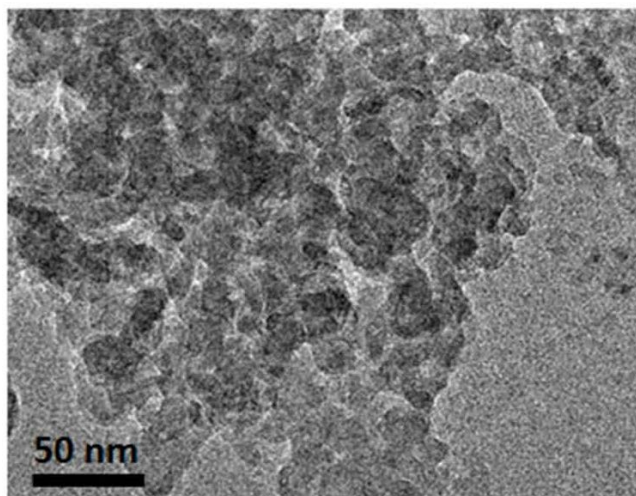
responds to Si-O-Si asymmetric stretching mode and its sharpness changes with method of calcination process. In addition, the bands at 800 cm<sup>-1</sup> and 465 cm<sup>-1</sup> are assigned to symmetric stretching and rocking vibration of Si-O-Si bonds, respectively. The presence of non-bridging oxygen (NBOs) atom is evidenced by the vibrational mode at 970 cm<sup>-1</sup> in both glasses.

The BET surface area and other relevant textural parameters of both glass samples were determined by nitrogen adsorption and desorption method, which are depicted in Figure 2. The 67SQNC glass sample shows the isotherm is of type IV with leveling off near saturation vapor pressure by indicating that the obtained glass sample possesses the mesoporous structure. The pore size distribution curves are obtained from the adsorption branch of isotherm using BJH model, which results in a narrow range and monomodal type distribution. Interestingly, we find a different type of isotherm in the case of 67SQMWC calcined sample, where we observe a type IV isotherm typical for mesoporous material with H2 type hysteresis loop characteristics of cylindrical pore structure. However, the obtained pore size distribution curve indicates a bimodal distribution with relatively small sizes between 4.6 and 6 nm. Furthermore, we have carried out the t-method of analysis on both samples to confirm the absence of micropores in the investigated samples [27] and the estimated corresponding textural parameters are listed in Table 1.

In Figure 3 we represent TEM images on both the glass samples, identifying a wormhole-like mesoporous structure and do not observe any ordered pore structure. The pH values of the SBF solution increase from its initial value after immersing the virgin glass sample for different periods due to the strong ion exchange process on the MBGs surface. The alkali and alkaline-earth cations near the glass surface get exchanged with H<sup>+</sup> or H<sub>3</sub>O<sup>+</sup> from the solutions, which lead to the rise in the pH values of the SBF solution [28]. However, we have found that after the initial sharp pH increase to 7.8 from 7.4 within the first 12 hrs of immersion in SBF and then it remains constant exceeding one day immersion in the case of 67SQNC glass sample as shown in Figure 4. On the other hand, 67SQMWC shows fast dissolution kinetics by observing the increase of pH value to 7.9 from its value followed by a decrease, which is attributed to the supe-



(A)



(B)

**Figure 3:** TEM images of (A) 67SQNC and (B) 67SQMWC pristine glass sample.

rior textural properties. Thus, the resulting pH value of the SBF solution strongly depends on the textural properties, buffering capacity of surrounding solution and the glass constituent [29].

In Figure 5, we show the XRD results on SBF soaked glass sample with different durations and the corresponding HCA formation. After immersion of the glass sample in SBF at different intervals, we observe significant changes in the virgin glass structure. In the case of 67SQNC sample, the glass structure is modified substantially with time and the observed diffraction peaks corresponds to the apatite-like layer of HCA phase within 12 hours of immersion in SBF. However, we observe different behavior in 67SQMWC glass sample where the obtained XRD pattern clearly shows the formed apatite phase co-exists

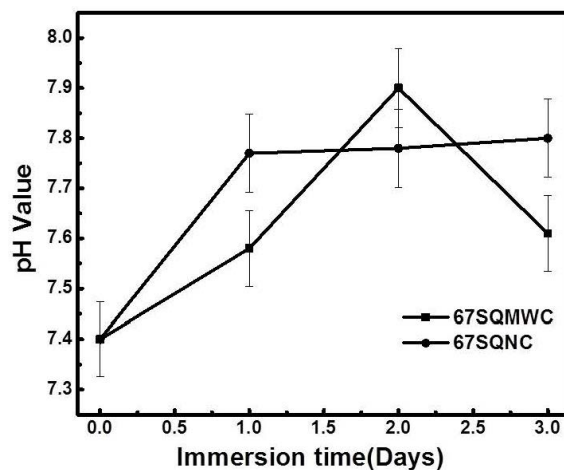


**Figure 4:** The variation of pH values SBF solution as a function of soaking time.

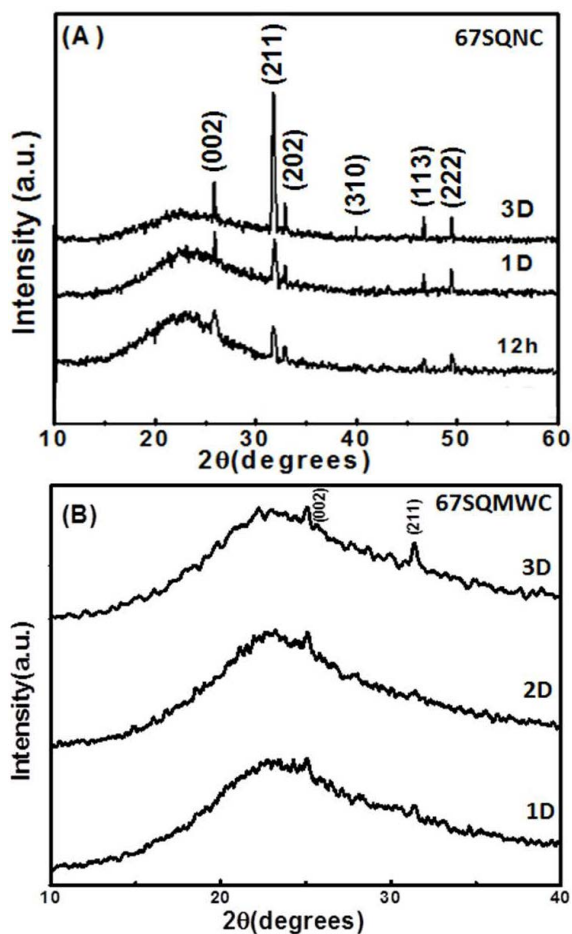


**Figure 5:** XRD pattern of (A) 67SQNC glass soaking in SBF for 12 h, 1D and 3D (B) 67SQMWC glass soaking for 1D, 2D and 3D.

in amorphous and crystalline states. More evidently, the formation of HCA phase is clear in the FTIR spectra obtained on different intervals as shown in Figure 6. The

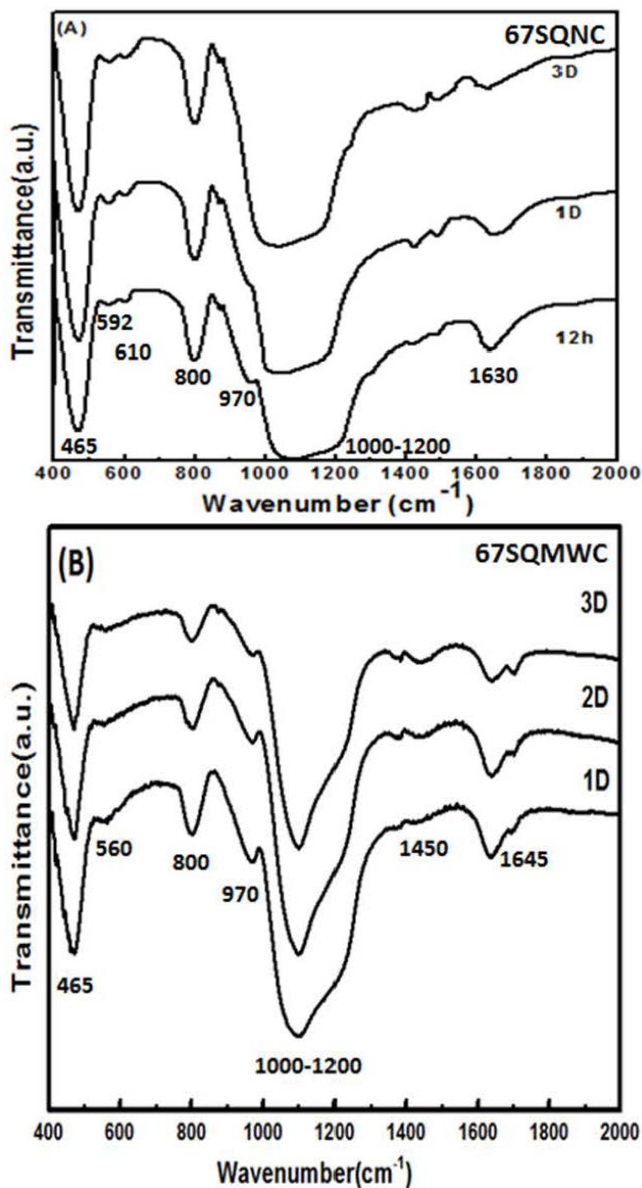


**Figure 6:** FTIR Spectra of (A) 67SQNC glass sample after soaked for 12 hours, 1D and 3D (B) 67SQMWC glass sample after being immersed in SBF for 1D, 2D and 3D.

spectra obtained on both glass sample show the broad band at  $1630\text{ cm}^{-1}$  corresponds to the formation of hydroxyl groups on the surface. The observed weak intensity peak at  $560\text{ cm}^{-1}$  indicates the presence of calcium phosphate cluster either in amorphous or crystalline state on the silica surface. Additionally, the absorption doublet band at  $592\text{ cm}^{-1}$  and  $610\text{ cm}^{-1}$  are characteristic of  $(\text{PO}_4)^{3-}$  units along with vibrations of P-O-Ca and P-O-P bands at  $670\text{ cm}^{-1}$  and  $748\text{ cm}^{-1}$ , respectively. On the basis of these results, we ascertain the formation of HCA phase in the SBF soaked mesoporous glass samples. Although the

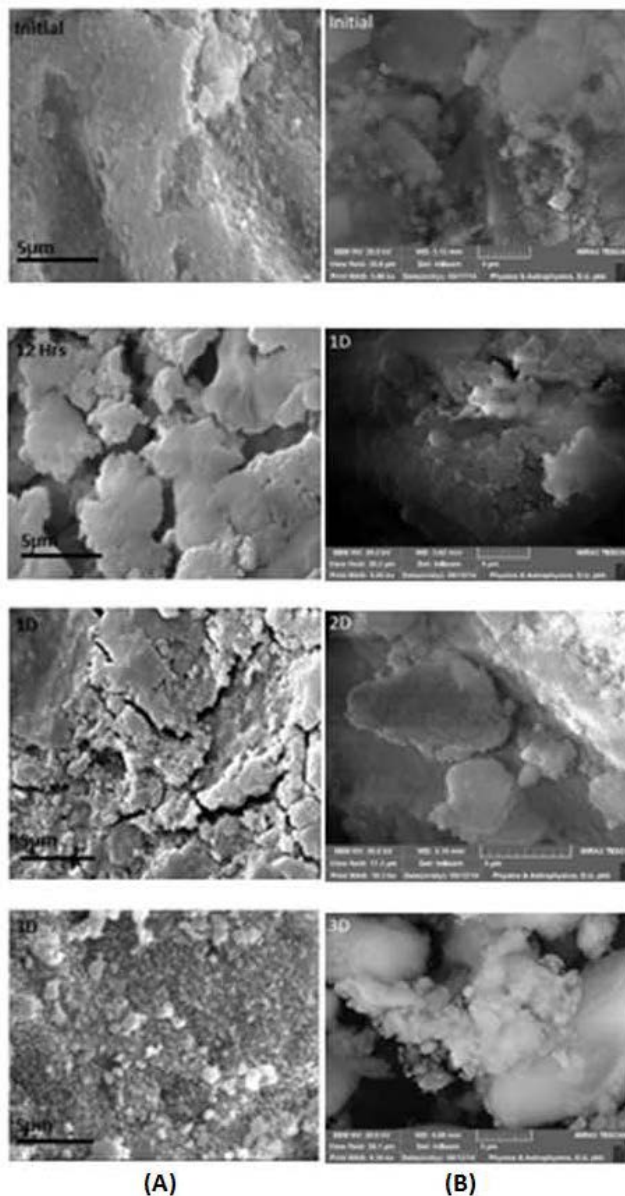


**Figure 7:** (A) SEM micrographs of 67SQNC glass before and after soaking for 12 hours, 1 and 3 days. (B) FESEM micrographs of 67SQMWC glass before and after soaking for 1, 2 and 3 days.

nature of HCA phase is different in both samples, their fast growth in 67SQMWC sample can't be neglected. Figure 7 shows the FESEM micrographs of as synthesized mesoporous 67SQNC and 67SQMWC glass samples with different soaking intervals. The FESEM micrograph of as synthesized 67SQNC glass powder show the smooth surface, whereas in 67SQMWC glass sample reveals the spongy surface typical of mesoporous glass samples. However, the obtained micrograph results show the surface morphology changes with SBF soaking period in both glass samples. However, the rate of formation of mineralized HCA

phase is much lower in the case of 67SQNC sample than 67SQMWC sample, which indicates the influence of textural characteristics on the dissolution of mesoporous BGs.

## 4 Discussions

The solid state synthesis using the microwave irradiation method is basically different from the conventional synthesis (*e.g.* coil heating method) because the heat is generated internally within the suspension/medium instead of supplying from the external source. In addition, the microwave heating method provides higher spatial distribution of heat as well as better heat-transfer rate, which ultimately lead us to obtain homogeneous pore sized glass particles. The combined BET surface area analysis and FE-SEM micrograph on the obtained powdered sample clearly show the significant difference in the morphology in comparison with as prepared glass sample. The high surface area and mesopore characteristics show the applicability of microwave calcination method for synthesizing the bioactive glasses without any nano or micro crystallites. It is interesting to observe that the obtained nitrogen adsorption-desorption isotherm exhibit distinct behavior in both the glass samples. In the case of 67SQNC sample which exhibit the H1 type hysteresis loop, *i.e.* it represents the one dimensional cylindrical pores, whereas H2 type of hysteresis loop corresponding to the ink bottle type of pores in 67SQMWC glass sample. As mentioned above, the main advantage of microwave method is that it provides very narrow and smaller sized pores than those of conventional heating method.

In addition to the superior textural characteristics, we find distinct behavior of biomineralization in both the mesoporous glass samples confirmed by the XRD and FTIR studies. On comparing the XRD pattern obtained on the 67SQNC glass sample with different period of SBF soaking, where it exhibits sharp Bragg reflections that corresponds to an apatite-like phase within 12 h of immersion in SBF (JCPDS number 09-0432). Whereas 67SQMWC glass sample with high surface area and narrow pore sizes, the formed HCA layer remains in amorphous state with minor amount of crystalline phase. The difference in behavior of biomineralization process in these two glass sample with different textural properties having similar chemical compositions can be understood in the following way. In general, the biomineralization processes are divided fundamentally into two different categories, namely (i) biologically induced and (ii) biologically controlled or organic matrix-mediated [30]. In both the cases, the nucle-

ation and growth process to occur within biological fluid medium, the biomineral formation requires a confined zone that attains and maintained by a sufficient supersaturation. The observed biomineralization process in 67SQNC sample is due to the rapid supersaturation followed by the nucleation and growth process. The supersaturation behavior SBF medium is supported by the independent pH measurement (see the Figure 4).

On the other hand, the 67SQMWC glass sample possesses the superior textural properties and lead to accelerated dissolution of the glass particle brings the unsaturated medium. However, the prolonged SBF soaking of BGs lead to the formation minor amount crystalline phase encapsulated with amorphous region. Recently, it has been reported in different binary, ternary and quaternary silicate glasses that the rapid biomineralization of formed amorphous HCA layer is highly influenced by the textural properties and chemical composition [31–33]. The present observation further indicates that the MBGs can induce the rapid formation of HCA layer but the biomineralization behavior is highly influenced by the supersaturation of the biological medium. In addition to the supersaturation behavior, the ionic strength mediates the charges of originator molecules, thus affecting the stabilizing the colloids and amorphous gels.

## 5 Conclusions

In summary, the present work describes the synthesis of a novel mesostructured bioactive glass formed by sol-gel process followed by microwave calcination. Additionally, we have shown the role of microwave irradiation on the morphological, structural, textural properties for a particular quaternary silicate glass composition and compared with conventionally calcined glass sample. The microwave calcined glass sample shows superior textural characteristics including the surface area, pore size and pore volume. The *in vitro* bioactivity assays have shown a rapid HCA formation on the surface of mesoporous bioactive glass sample with distinct behavior of biomineralization in both glass samples. The observed difference in the biomineralization process has been discussed in terms of their chemical kinetics of supersaturation of the biological medium. The present results indicate that this novel method of calcination offers a synergy to obtain superior textural characteristic BGs, enhancing its potential for bone tissue regeneration purposes.

**Acknowledgement:** We acknowledge USIC, University of Delhi for providing the characterization facilities for experimental work. One of us (AK) is thankful to University Grant Commission (UGC) for providing the Junior Research Fellowship (JRF).

## References

- [1] Jones J.R., Gentleman E., Polak J., Bioactive glass scaffolds for bone regeneration, *Elements*, 2007, 3, 393-399
- [2] Albrektsson T., Johansson C., Osteoinduction, osteoconduction and osseointegration, *Eur Spine J.*, 2001, 10, S96-S101
- [3] Chen Q.Z., Thouas G.A., Fabrication and characterization of sol-gel derived 45S5 bioglass ceramics scaffolds, *Acta. Biomater.*, 2011, 7, 3616-3626
- [4] Chen Q.Z., Xu J.L., Yu L.G., Fang X.Y., Khor K.A., Spark plasma sintering of sol-gel derived 45S5 bioglass ceramics: mechanical properties and biocompatibility evaluation, *Mater. Sci. Eng. C*, 2012, 32, 494-502
- [5] Pirayesh H., Nychka J.A., Sol-gel synthesis of bioactive glass-ceramics 45S5 and its in vitro dissolution and mineralization behavior, *J. Am. Ceram. Soc.*, 2013, 96, 1643-1650
- [6] Wu C., Luo Y., Cuniberti G., Xia Y., Gelinsky M., Three dimensional printing of hierarchical and tough mesoporous bioactive glass scaffolds with controllable pore architecture, excellent mechanical strength and mineralization ability, *Acta. Biomater.*, 2011, 7, 2644-2650
- [7] Fu Q., Rahaman M.N., Bal B.S., Brown R.F., Day D.E., Mechanical and in vitro performance of 13-93 bioactive glass scaffolds prepared by a polymer foam replication technique, *Acta. Biomater.*, 2008, 4, 1854-1864
- [8] Pena J., Roman J., Cabanas M.V., Vallet-Regi M., An alternative technique to shape Scaffolds with hierarchical porosity at physiological temperature, *Acta. Biomater.*, 2010, 6, 1288-1296
- [9] Mallick K.K., Freeze casting of porous bioactive glass and bioceramics, *J. Am. Chem. Soc.*, 2009, 92 [S1], S85-S94
- [10] Yan X., Huang X., Yu C., Deng H., Wang Y., Zhong Z., Qiao S., Lu G., Zhao D., The in-vitro bioactivity of mesoporous bioactive glasses, *Biomater.*, 2006, 27, 3396-3403
- [11] Xia W., Chang J., Well-ordered mesoporous bioactive glasses (MBG): a promising bioactive drug delivery system, *J. Cont. Rel.*, 2006, 110, 522-530
- [12] Yun H.S., Kim S.E., Hyun Y.T., Heo S.J., Shin J.W., Hierarchically mesoporous-macroporous bioactive glasses scaffolds for bone tissue regeneration, *J. Biomed. Mater. Res. B: Appl. Biomater.*, 2008, 87B, 374-380
- [13] Yun H.S., Kim S.E., Hyeon Y.T., Design and preparation of bioactive glasses with hierarchical pore networks, *Chem. Comm.*, 2007, 21, 2139-2141
- [14] Li X., Wang X., Chen H., Jiang P., Dong X., Si J., Hierarchically porous bioactive glass scaffolds synthesized with a PUF and P123 contemplated approach, *Chem. Mater.*, 2007, 19, 4322-4326
- [15] Zhu Y., Wu C., Ramaswamy Y., Kockrick E., Simon P., Kaskel S., Zreiqat H., Preparation, characterization and in vitro bioactivity of mesoporous bioactive glasses (MBGs) scaffolds for bone tissue engineering, *Micropor. Mesopor.*, 2008, 112, 494-503
- [16] Brinker C.J., Lu Y., Sellinger A., Fan H., Evaporation-induced self-assembly: nanostructures made easy, *Adv. Mater.*, 1999, 11, 579-585
- [17] Shih C.C., Chien C.S., Kung J.C., Chen J.C., Chang S.S., Lu P.S., Shih C.J., Effect of surfactant concentration on characteristics of mesoporous bioactive glass prepared by evaporation induced self-assembly, *Appl. Surf. Sci.*, 2013, 264, 105-110
- [18] Li X., Shi J., Dong X., Zhang L., Zeng H., A mesoporous bioactive glass/polycaprolactone composite scaffold and its bioactivity behavior, *J. Biomed. Mater. Res. A*, 2008, 84A, 84-91
- [19] Alcaide M., Portoles P., Noriega A.L., Arcos D., Vallet-Regi M., Portoles M.T., Interaction of an ordered mesoporous bioactive glass with osteoblasts, fibroblasts and lymphocytes, demonstrating its biocompatibility as a potential bone graft material, *Acta. Biomater.*, 2010, 6, 892-899
- [20] Noriega A.L., Arcos D., Barba I.I., Sakamoto Y., Terasaki O., Vallet-Regi M., Ordered mesoporous bioactive glasses for bone tissue regeneration, *Chem. Mater.*, 2006, 18, 3137-3144
- [21] Yan X.X., Deng H.X., Huang X.H., Lu G.Q., Qiao S.Z., Zhao D.Y., Yu C.Z., Mesoporous bioactive glasses I. synthesis and structural characterization, *J. Non-Cryst. Solids*, 2005, 351, 3209-3217
- [22] Hoppe A., Guldel N.S., Boccaccini A.R., A review of the biological response to ionic dissolution products from bioactive glasses and glass-ceramics, *Biomater.*, 2011, 32, 2757-2774
- [23] Vaid C., Murugavel S., Alkali oxide containing mesoporous bioactive glasses: synthesis, characterization and in vitro bioactivity, *Mater. Sci. Eng C*, 2013, 33, 959-968
- [24] Vaid C., Murugavel S., Kashayap R., Tandon R.P., Synthesis and in vitro bioactivity of surfactant templated mesoporous sodium silicate glasses, *Micropor. Mesopor. Mater.*, 2012, 159, 17-23
- [25] Kokubo T., Takadama H., How useful is SBF in predicting in vivo bone bioactivity?, *Biomater.*, 2006, 27, 2907-2915
- [26] Aguiar H., Serra J., Gonzalez P., Leon B., Structural study of sol-gel silicate glasses by IR and Raman spectroscopies, *J. Non-Cryst. Solids*, 2009, 355, 475-480
- [27] Bhamhani M.R., Cutting P.A., Sing K.S.W., Turk D.H., Analysis of nitrogen adsorption isotherms on porous and nonporous silicas by the BET and  $\alpha$ s methods, *J. Colloid Interface Sci.*, 1972, 308, 109-117.
- [28] Horcajada P., Ramila A., Boulahya K., Gonzalez-Calbet J., Vallet-Regi M., Bioactivity in ordered mesoporous materials, *Solid State Sci.*, 2004, 6, 1295-1300.
- [29] Du Min Q., Bian Z., Jiang H., Greenspan D.C., Burwell A.K., Zhong J., Tai B.J., Clinical evaluation of a dentifrice containing calcium sodium phosphosilicate (novamin) for the treatment of dentin hypersensitivity, *Am. J. Dent.*, 2008, 21, 210-214.
- [30] Weiner S., Dove P.M., An overview of biomineralization processes and the problem of the vital effect, *Rev. Mineral. Geochem.*, 2003, 54, 1-29
- [31] Garcia A., Cicuendez M., Barba I.I., Arcos D., Vallet-Regi M., Essential role of calcium phosphate heterogeneities in 2D-hexagonal and 3D-cubic SiO<sub>2</sub>-CaO-P<sub>2</sub>O<sub>5</sub> mesoporous bioactive glasses, *Chem. Mater.*, 2009, 21, 5474-5484
- [32] Yan H., Zhang K., Blandford C.F., Francis L.F., Stein A., In vitro hydroxycarbonate apatite mineralization of CaO-SiO<sub>2</sub> sol-gel glasses with a three-dimensionally ordered macroporous structure, *Chem. Mater.*, 2001, 13, 1374-1382
- [33] Salinas A.J., Martin A.I., Vallet-Regi M., Bioactivity of three CaO-P<sub>2</sub>O<sub>5</sub>-SiO<sub>2</sub> sol-gel glasses, *J. Biomed. Mater. Res. A*, 2002, 61, 524-532